Planta (2007) 226:981–987
DOI 10.1007/s00425-007-0544-9

ORIGINAL ARTICLE

Tensile and compressive stresses in tracheids are induced by swelling based on geometrical constraints of the wood cell

Ingo Burgert · Michaela Eder · Notburga Gierlinger · Peter Fratzl

Received: 12 January 2007 / Accepted: 27 April 2007 / Published online: 7 June 2007
© Springer-Verlag 2007

Abstract Plants are able to pre-stress their tissues in order to actuate their organs. Here, we demonstrate with two tissue types of the secondary xylem of conifers (normal wood and compression wood of spruce (*Picea abies*)) that either tensile or compressive stresses can develop in the longitudinal direction during the swelling of the cell wall. This dramatic difference appears to be due mostly to differences in cell geometry and cellulose fibril orientation. A mechanical model was developed to demonstrate swelling experiments with the help of sodium iodide experiments. The reversal of longitudinal extension can be predicted, based on the orientation of the (nearly inextensible) cellulose fibrils and the shape of the cell.

Keywords Cell wall · Conifers · Growth stress generation · Mechanical modeling · Swelling treatment · Tracheids

Introduction

How conifers generate either tensile or compressive stresses in their cells according to needs is a long-standing question, which could not yet be fully resolved. In a straight trunk, the outer part of the secondary xylem is pre-stressed in tension in the longitudinal direction (Boyd 1950a; Kubler 1987). These longitudinal tensile stresses are essential to withstand high wind loads, since they compensate for the comparatively low compressive strength of the wood structure (Mattheck and Kubler 1996). In addition to these ''normal'' wood tissues, conifers build up compression wood that directs growing organs towards a predetermined position. As the name implies, this tissue type generates longitudinal compressive stresses in its cells and can be found at the underside of leaning stems and branches (Wardrop 1965).

Macroscopic properties and pre-stresses in wood mainly originate from the levels of cell and cell wall organisation due to the hierarchical structure (Fig. 1).

The cell wall of the prosenchymatic cells (tracheids) consists of nanometer-thick cellulose fibrils, which are embedded in an amorphous matrix of hemicelluloses and lignin (Fengel and Wegener 1984; Fahlén and Salmén 2005). The normal adult wood tracheid of a straight trunk is almost rectangular and the cellulose fibrils in the thickest cell wall layer are oriented in a steep helical curve resulting in a rather low microfibril angle in the order of ~10° which measures the spiral angle of the cellulose fibrils with the axial cell direction.

The round compression wood tracheids have a much higher microfibril angle in the order of ~45° and a different chemical composition compared to normal wood cells (Côte and Day 1965; Timell 1982). The mechanical performance of each cell type is significantly influenced by the orientation of the helically wound cellulose fibrils (Reiterer et al. 1999) resulting in stiff and strong normal wood cells and flexible but tough compression wood cells.

Despite the importance of growth stress generation for the biomechanics of trees, the underlying mechanisms have not been clarified. It is a fact that for living plant cells (as opposed to dead wood cells) spatial gradients in water potential can be generated actively, in order to pre-stress the tissues and allow for organ movement (e.g. Venus flytrap) (Braam 2005; Forterre et al. 2005). For the opening of pine cones, Dawson et al. (1997) showed that moisture

I. Burgert (✉) · M. Eder · N. Gierlinger · P. Fratzl
Department of Biomaterials, Max Planck Institute of Colloids and Interfaces, 14424 Potsdam, Germany
e-mail: ingo.burgert@mpikg.mpg.de

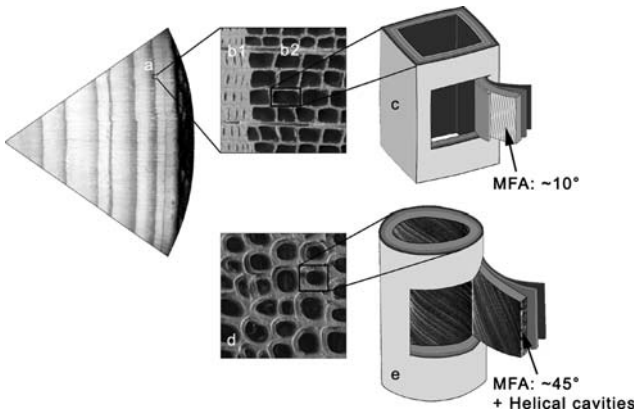

Fig. 1 Structure of tracheids in spruce (*Picea abies*). *a* Growth rings. *b1*, *b2* Latewood and earlywood of normal tissue, respectively. *c* Normal wood cell with square shape and a small microfibril angle (*MFA*) in the order of ~10°. *d* Compression wood tissue. *e* Round compression wood cell with a microfibril angle in the order of ~45° and helical cavities on the inner side of the cell wall parallel to the cellulose fibrils

changes could actuate specific movements even in dead tissues.

In living conifers, the tracheids die at the end of their differentiation process when secondary cell wall layers have been formed. Hence, internal stresses have to be incorporated in the cell wall during differentiation before cell senescence. Common hypotheses on growth stress generation emphasise the retarded insertion of constituents during cell wall formation (Boyd 1950b; Bamber 1979). Indeed, lignification is taking place with a time delay compared to cellulose and hemicelluloses agglomeration (Boerjan et al. 2003). Hence, a swelling of the cell wall during lignification (Boyd 1950b) or an influence of lignin agglomeration on cellulose crystallisation (Bamber 1979) was supposed. But it has been shown that none of these hypotheses could explain the controlled generation of both either tensile or compressive stresses (Yamamoto 1998).

Combined approaches, integrating empirical data and modeling, have been used previously to explore the constraints that govern the complex structural design of trees during growth and development (McMahon 1973; Niklas and Spatz 2004). In the present work, we use measurements of the elongation of wet cells and tissues of normal and of compression wood in a saturated sodium iodide solution to devise a mechanical model for cell deformation based upon cell wall swelling. Our findings suggest that conifers are able to generate either tensile or compressive stresses simply by slightly modulating cell geometry and cell wall ultrastructure, in particular the orientation of cellulose microfibrils in the secondary cell wall layer.

Materials and methods

Wet, never-dried wood samples of spruce [*Picea abies* (L.) Karst.] were stored in a saturated sodium iodide solution for an additional swelling of the cell wall beyond the fibre saturation point. The salt penetrates into the wood cell walls and increases the water amount that can be adsorbed by the porous material. Sorption isothermes show that the moisture content of salt-treated wood is distinctly higher than the moisture content of normal wood (Loughborough 1937, cited in Kollmann 1982).

Single tracheids were isolated mechanically under a light microscope from ~150-μm-thick tangential wood sections by using very fine tweezers (Burgert et al. 2005). These never-dried cells were stored in distilled water on an object slide under a cover slip and were treated with the saturated sodium iodide solution for 2 h. The longitudinal lengths of 10 normal wood and 11 compression wood cells were measured before and after treatment. Further experiments were conducted on radial and tangential tissue sheets of normal wood and compression wood as well as bulk wood using normal wood cuboids. The wet tissue slices had a longitudinal length of ~30 mm, a width of ~4 mm and a thickness of 150–190 μm in the tangential and in the radial direction, respectively. For each category five specimens were stored in the saturated sodium iodide solution for 3 days. The lengths of the tracheids and of the tissues were measured by making several consecutive images at high magnification and finally reassembling them into one.

The normal wood blocks had a longitudinal length of ~40 mm, a tangential length of ~16 mm and a radial length of ~10 mm. Five specimens were stored in the saturated salt solution for 2 months. The length of the axes was measured using a calliper. Calliper measurements on compression wood blocks were not meaningful because of a distinct distortion of their shape due to the sodium iodide treatment.

Cellulose microfibril angles were determined on the tissue sections that had served for the tracheid isolation. The microfibril angles of the tissue sections were measured to be 12° for normal wood and 52° for compression wood (determined by X-ray scattering; Lichtenegger et al. 1999), which was in well agreement with measurements by Reiterer et al. (1999).

A bilayer consisting of a normal wood and a compression wood tissue of ~200 μm thickness was prepared by gluing together the wet samples using cyanoacrylate glue. The deformation upon swelling with sodium iodide was recorded.

For imaging lignin distribution 2D spectral maps were acquired from 10-μm-thick cross sections of spruce opposite (geometrically close to normal wood) and compression wood with a Confocal Raman Microscope (CRM200,

Witec, Ulm, Germany). Equipped with an objective from Nikon [x 60, numerical aperture (NA) = 0.80] a linear polarised laser (diode pumped Green laser, λ = 532 nm, CrystaLaser) was focused with a diffraction limited spot size (0.61 λ/NA) and the Raman light detected by an air-cooled, back-illuminated spectroscopic CCD (Andor, Belfast, North-Ireland) behind a grating (600 g mm^{-1}) spectrograph (Acton, Princeton Instruments Inc., Trenton, NJ, USA). On a sampling area of 30 × 30 µm^2 every 0.47 µm a spectrum was recorded with an integration time of 2 s and lignin distribution was followed according to Gierlinger and Schwanninger (2006).

Results

Swelling experiments

The treatment of mechanically isolated tracheids, radial and tangential slices of normal wood and compression wood as well as bulk wood samples of normal wood with a saturated sodium iodide solution changed the dimensions of the specimens (Fig. 2).

The compression wood cells were elongated by ~2.5%, whereas the normal wood cells showed a reduction in length by ~0.3%. Both radial and tangential compression wood slices showed an elongation in the longitudinal direction and moderate increases in transverse lengths, indicating a volume increase of the samples (Fig. 2b). In terms of the tangential normal wood slices a slight decrease in longitudinal length was observed accompanied by a pronounced increase in the tangential direction. The radial normal wood slices neither showed a significant change in the longitudinal nor in the radial direction (Fig. 2c). For the normal bulk wood an increase in volume was calculated, despite a longitudinal and a radial shortening of the samples. This directly opposed behaviour resulted from the superimposition by the pronounced tangential swelling (Fig. 2d).

Mechanical model

To relate the structural characteristics of the two cell types to their specific deformation during swelling, a mechanical model was developed based on the assumption that most of the deformation occurs in the interfibrillar matrix rather than in the comparatively rigid cellulose fibrils (Spatz et al. 1999; Keckes et al. 2003; Fratzl et al. 2004). Specifically, it was assumed (1) that the mechanical behaviour is dominated by the secondary wall, (2) that the cellulose is sufficiently stiff (in tension) compared to the matrix to consider it effectively inextensible (considering the fibrils extensible but much stiffer than the matrix would not change the main conclusions but would make the mathematical treatment less transparent), (3) that the cell wall matrix is elastically isotropic with Poisson coefficient ν and Young's modulus E_M and (4) is subjected to an isotropic-swelling strain of ε_0 ($3\varepsilon_0$ being the volume increase). Finally, (v) plane stress conditions for the cell wall were assumed.

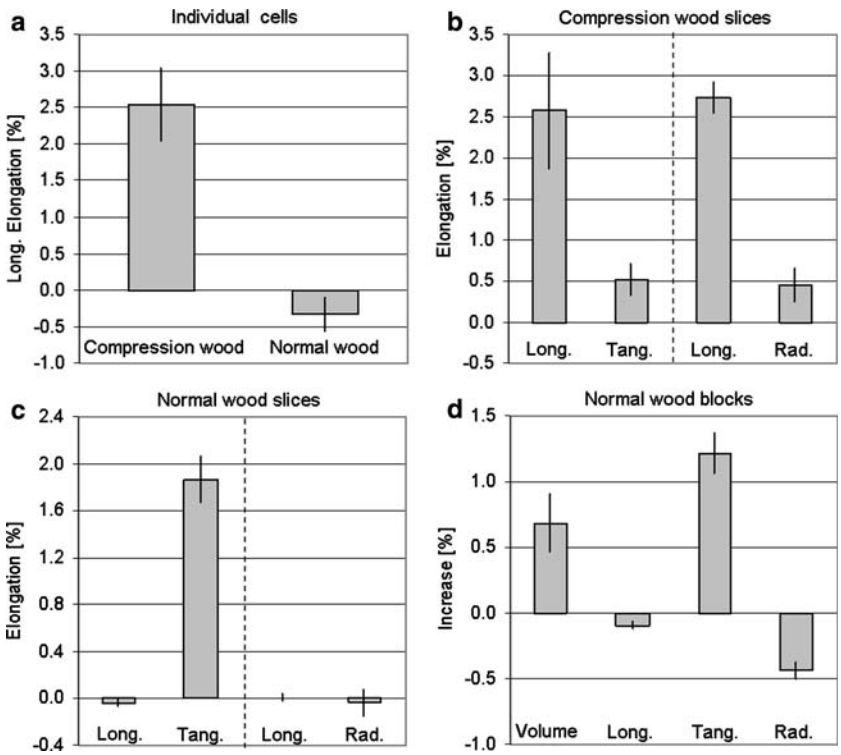

Fig. 2 Elongation of spruce wood dimensions during sodium iodide treatment. **a** Longitudinal extension of freestanding single wood cells; compression wood cells, n = 11; normal wood cells, n = 10. **b** Deformation of radial and tangential compression wood slices n = 5. **c** Deformation of radial and tangential normal wood slices n = 5. **d** Deformations in all directions of a bulk specimen (cuboids) of normal wood, n = 5. Longitudinal (*long.*), tangential (*tang.*) and radial (*rad.*) refer to the main axes in wood. Bar graphs show arithmetic means ± SD

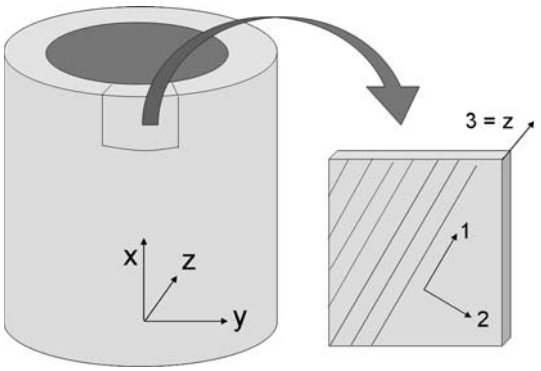

Fig. 3 Coordinate axes for the mechanical description of the cell wall. The cell may have any shape for this model (round or rectangular cross-section)

Two coordinate systems (Carlsson and Pipes 1989) were defined, one where x is parallel to the cell axis and z perpendicular to the cell wall (Fig. 3), and another, where 1 is parallel to the cellulose fibrils and 3 is perpendicular to the cell wall.

The microfibril angle between the cell axis and the cellulose fibril direction is denominated μ, and $m = \cos(\mu)$, $n = \sin(\mu)$. In the 1,2,3 coordinate system, the deformation of the isotropic matrix between the cellulose fibrils is written:

$$\varepsilon_i - \varepsilon_0 = \sum_{k=1}^{3} S_{ik}\sigma_k \quad \gamma_{ij} = \tau_{ij}/G, \quad \text{with} \quad i,j = 1,2,3 \quad \text{and} \quad i \neq j \tag{1}$$

where

$$S_{11} = S_{12} = S_{33} = \frac{1}{E_{\mathrm{M}}},$$
$$S_{12} = S_{13} = S_{23} = -\frac{\nu}{E_{\mathrm{M}}} = \frac{1}{E_{\mathrm{M}}} - \frac{1}{2G},$$
$$\frac{1}{G} = \frac{2(1+\nu)}{E_M}.$$

The action of the (inextensible) cellulose fibrils is described by the boundary condition $\varepsilon_1 = 0$. Moreover, the plane stress conditions mean that $\sigma_3 = \tau_{23} = \tau_{31} = 0$. The corresponding expressions for the compliance matrix in the rotated coordinate system (x,y,z) are identical to those in Eq. 1, since the matrix is supposed isotropic and only the boundary condition needs to be rotated. We define σ^{F} as the stress applied by the fibrils to the matrix. The value of this stress will be such that $\varepsilon_1 = 0$. Applying tensor rotation, this means that stresses of $m^2\ \sigma^{\mathrm{F}}$, $n^2\ \sigma^{\mathrm{F}}$ and $mn\sigma^{\mathrm{F}}$ (which the cellulose exerts onto the matrix) add to the external stresses σ_x, σ_y and τ_{xy}, respectively. As the plane stress conditions are conserved by rotation into the (x,y,z) frame, we only need to consider the stresses and strains as shown in the following matrix relation:

$$\begin{bmatrix}\varepsilon_x\\ \varepsilon_y\\ \gamma_{xy}\end{bmatrix} = \begin{bmatrix}\varepsilon_0\\ \varepsilon_0\\ 0\end{bmatrix} + \frac{1}{E_{\mathrm{M}}}\begin{bmatrix}1 & -\nu & 0\\ -\nu & 1 & 0\\ 0 & 0 & 2(1+\nu)\end{bmatrix} \times \begin{bmatrix}\sigma_x + m^2\,\sigma^{\mathrm{F}}\\ \sigma_y + n^2\,\sigma^{\mathrm{F}}\\ \tau_{xy} + mn\,\sigma^{\mathrm{F}}\end{bmatrix} = \begin{bmatrix}\varepsilon_x^0\\ \varepsilon_y^0\\ \gamma_{xy}^0\end{bmatrix} + \frac{1}{E_{\mathrm{M}}}\begin{bmatrix}M_{11} & M_{12} & M_{13}\\ M_{12} & M_{22} & M_{23}\\ M_{13} & M_{23} & M_{33}\end{bmatrix}\begin{bmatrix}\sigma_x\\ \sigma_y\\ \tau_{xy}\end{bmatrix} \tag{2}$$

with the constraint that $\varepsilon_1 = m^2\varepsilon_x + n^2\varepsilon_y + mn\gamma_{xy} = 0$.

This constraint allows to determine σ^{F} as

$$\sigma^{\mathrm{F}} = -E_{\mathrm{M}}\varepsilon_0 - (m^2 - \nu n^2)\sigma_x - (n^2 - \nu m^2)\sigma_y - 2mn(1+\nu)\tau_{xy}. \tag{3}$$

Reinserting into (Eq. 2) gives the matrix coefficients:

$$\begin{aligned} &M_{11} = n^2(1+\nu)(1+m^2-\nu n^2); && \varepsilon_x^0 = n^2(1+\nu)\varepsilon_0;\\ &M_{22} = m^2(1+\nu)(1+m^2-\nu m^2); && \varepsilon_y^0 = m^2(1+\nu)\varepsilon_0;\\ &M_{33} = 2(1+\nu) - 4m^2n^2(1+\nu)^2; && \gamma_{xy}^0 = -2mn(1+\nu)\varepsilon_0.\\ &M_{12} = -m^2n^2(1+\nu)^2;\\ &M_{13} = -2mn(1+\nu)(m^2-\nu n^2);\\ &M_{23} = -2mn(1+\nu)(n^2-\nu m^2); \end{aligned} \tag{4}$$

Four different boundary conditions may now be considered for the cell:

(1) $\varepsilon_y = \gamma_{xy} = 0$, no lateral swelling and no torsion of the wood cell is possible: from the boundary condition, it follows that $\varepsilon_x = 0$, independently of swelling or tensile stress. This means that there can be no growth stresses in this case.

(2) $\sigma_y = 0$, $\gamma_{xy} = 0$, torsion of the cell is inhibited, but lateral swelling is possible: one obtains in this case $\tau_{xy} = mn\frac{E_M\varepsilon_0 + (m^2-\nu n^2)\sigma_x}{1-2m^2n^2(1+\nu)}$, from which it follows that $\varepsilon_x = \frac{n^2(1+\nu)}{1-2m^2n^2(1+\nu)}\left((n^2-m^2)\varepsilon_0 + n^2(1-\nu)\frac{\sigma_x}{E_{\mathrm{M}}}\right)$. In particular, when the cell is inserted into a strong tissue, then $\varepsilon_{\mathrm{x}} = 0$ and the cell exerts a tensile stress of $\sigma_x = \frac{m^2-n^2}{(1-\nu)n^2}E_{\mathrm{M}}\varepsilon_0$ onto the tissue.

(3) $\varepsilon_y = 0$, $\tau_{xy} = 0$, no lateral swelling of the cell, but torsion is possible: here $\varepsilon_x = \frac{2n^2(1+\nu)}{1+n^2-\nu m^2}\left(\varepsilon_0 + (1-\nu)\frac{\sigma_x}{E_{\mathrm{M}}}\right)$ and in the tissue ($\varepsilon_x = 0$), the cell exerts a compressive stress $\sigma_x = -\frac{E_{\mathrm{M}}\varepsilon_0}{1-\nu}$.

(4) $\sigma_{\mathrm{y}} = \tau_{\mathrm{xy}} = 0$, free cell (lateral swelling and torsion possible): here $\varepsilon_x = n^2(1+\nu)\varepsilon_0 + n^2(1+\nu)$

$(1 + m^2 - \nu n^2)\frac{\sigma_x}{E_M}$ and, in the tissue ($\varepsilon_x = 0$), the cell exerts a compressive stress (quite similar to case c) of $\sigma_x = -\frac{E_M \varepsilon_0}{1+m^2-\nu n^2}$.

In consequence, a newly formed tracheid added to the existing wood tissue puts quite a different stress on the wood tissue when its cell wall matrix is swelling, depending on the condition (2), on the one hand, and (3) or (4) on the other. For a cell where torsion is inhibited (case 2), the stress is tensile (corresponding to a shortening of the cell) and depends strongly on microfibril angle as $\sigma_x = \frac{(\cot \mu)^2 - 1}{(1-\nu)} E_M \varepsilon_0$.

The longitudinal stress developed for a given swelling increases when the microfibril angle gets smaller. As a consequence, the largest tensile stresses are developed for small microfibril angles. However, for a cell where (small) torsional deformation is possible (cases 3 or 4), the stress is compressive and only weakly dependent on the microfibril angle. Typically the stress is between $-E_M\varepsilon_0/(1 - \nu)$ and $-E_M\varepsilon_0/2$.

The calculations point out an interesting geometrical constraint on the cell, which is schematically shown in Fig. 4. In fact, two cases have to be distinguished, where (some) torsion of the cells is allowed and where this is completely forbidden. The behaviour in the second case is shown in Fig. 4c.

No torsion means that the rectangular cell wall sheet (obtained after virtually cutting the cell along a vertical line) has to remain rectangular. The challenge is now to increase the surface of the rectangle keeping the length of the diagonal (thick line in Fig. 4b–d) fixed. It is mathematically easy to show that the rectangle with the largest area at fixed diagonal length is a square. Hence, for a microfibril angle of less than 45°, the only way to increase the area (and, thus, to swell the matrix) is to shorten the cell in longitudinal direction. However, if some torsion is allowed the matrix swelling results in a longitudinal elongation (Fig. 4d).

The distribution of lignin in cell walls of both, the upper and lower side of a branch, is shown by Confocal Raman microscopy (Fig. 5).

Similarly, as in normal wooden cells, in the opposite wood tracheids of the upper part the highest lignin concentrations occur in the middle lamella and primary wall (Fig. 5a), whereas in the compression wood tracheids of the lower part an outer ring of less lignin is found at the cell interfaces (Fig. 5b).

Discussion

The sodium iodide treatments and the mechanical modeling consistently indicated an opposite deformation response of water-saturated cell walls of compression wood and normal wood tracheids upon additional swelling.

Compression wood tracheids and both tissue slices showed an increase in longitudinal length after the swelling treatment. In terms of normal wood, the individual cells, the tangential slices and the bulk wood samples shrank in the longitudinal direction.

However, the radial slices of normal wood did not show a change in the longitudinal and radial direction. Both, the exceptional behaviour of the radial normal wood slices and the radial shrinkage of the bulk wood samples cannot be interpreted by the deformation of the individual tracheid but might be explained by considering the influence of rays at the tissue level. They may tend to shrink in their axial direction and prevent the tracheids from swelling in the radial direction or even induce radial tissue shrinkage. In the living tree, the radial-oriented wood rays can generate radial tensile stresses (Burgert et al. 2003). In the swelling experiments they might be able to cause a transverse anisotropy at the tissue level consistently, apparent in a radial contraction of the normal bulk wood samples and an exceptional behaviour of the radial normal wood tissues slices.

The opposite deformation of normal wood and compression wood and the mechanical model showed that depending on the cell type either tensile or compressive stresses can develop in the longitudinal direction of wood cells from spruce. Most importantly, this occurred despite

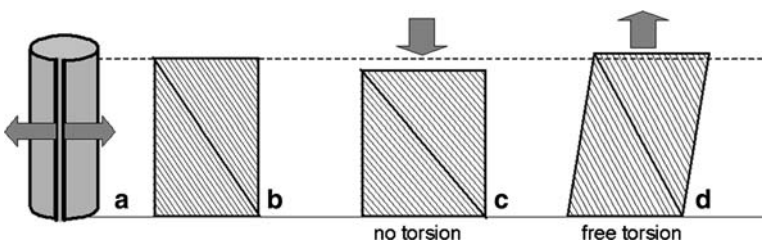

Fig. 4 Deformation of the cell wall during swelling with inextensible cellulose fibrils (example with microfibril angle = 30°). **a** Cell virtually cut open along a vertical line. **b** Cell wall rolled out with microfibrils. **c** Increase of cell wall area due to swelling when the length of the fibrils is kept fixed and no torsion of the cell is allowed. **d** Same when torsion of the cell is allowed. The thick line highlights on the cellulose fibrils crossing the piece of cell wall along a diagonal. This line has to keep the same length during swelling

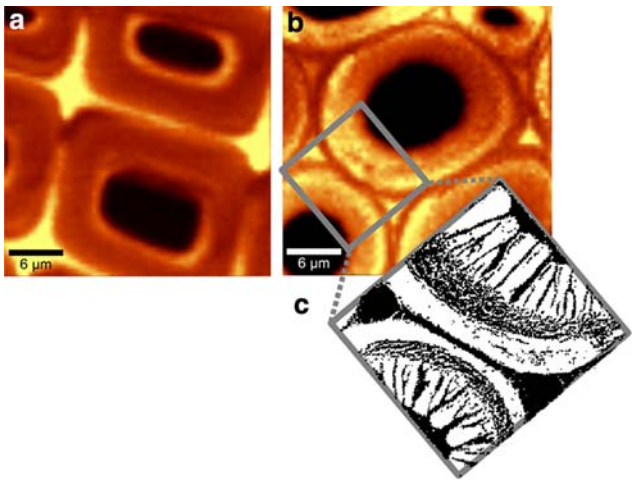

Fig. 5 Raman spectroscopic images showing cell shape and lignin distribution in wood cells on the upper and lower side of a branch (*yellow* = high lignin content, *dark* = low). **a** Opposite wood (almost same cell shape and lignin distribution as normal wood). **b** compression wood. **c** Enlarged image of a cell wall emphasising the helical cavities (after Timell 1982)

the fact that the cell wall was swelling in both cases which indicates that the different structural designs of the two types of cells are crucial factors. The significance of these observations for the biomechanics of organ actuation in the living tree depends on two crucial aspects:

1. the theoretical considerations have to coincide with the microstructural features of normal and compression wood cells and
2. the stresses generated upon swelling have to actuate a bending process or organ movement, respectively.

Normal wood cells (or the so-called opposite wood in branches as shown in Fig. 5) have a nearly rectangular or hexagonal cell shape. As a consequence, a torsional movement is almost eliminated and, therefore, the small microfibril angle in the order of ~10° explains why the cell is shrinking longitudinally when the matrix is swelling. By contrast, compression wood cells do not have a square shape, but are essentially round and can have helical cavities running parallel to the cellulose fibrils (see Figs. 1, 5). Therefore, the constraint of no torsional deformation is somewhat relaxed.

Moreover, the distribution of lignin (which contributes to stiffen the matrix) as shown by Confocal Raman Microscopy (Fig. 5) coincides with the structural constraints. In normal wood cells (or opposite wood cells) the compound middle lamella (middle lamella and primary wall) is heavily lignified, reducing the ability of cells to deform against each other in shearing. Contrarily, in the compression wood cells an outer ring of low lignin content (Fig. 5b) helps to provide (small) torsional deformation of the cell. As a consequence, the boundary conditions are expected to be different in this case and correspond to case d in Fig. 4.

By balancing the stress distribution in trunks and branches, conifers are able to protect the trunks from failing on the compression side and to keep upright their leaning stems and branches. For the latter, we assume a concerted stress generation strategy for the upper and lower parts of the organ in the living tree which is demonstrated by a model system of a bilayer consisting of a normal wood and a compression wood tissue (Fig. 6).

The wood tissues were glued together in wet state. An additional swelling by sodium iodide resulted in an axial elongation of the compression wood side and an axial shrinking of the normal wood side (see Fig. 2). As a consequence the bilayer bent towards the normal wood side. Hence, in the living tree the action of the compression wood tissues can be enhanced by high-tensile stresses generated on the upper side by rectangular wood cells with lower microfibril angle (Färber et al. 2001).

For calculating the amount of growth stresses, usually cuts are made into the secondary xylem of the standing trees and the release of strains is measured for instance by strain gauges. The dimensional changes of the normal bulk wood samples upon the swelling treatment (Fig. 2d) are in good coincidence with growth stresses that are examined in the longitudinal, tangential and radial direction of the outer xylem of a straight trunk (normal wood) (Boyd 1950a; Kubler 1987; Mattheck and Kubler 1996).

Typical strains released in the longitudinal direction are ~ –0.04% in normal wood and ~ +0.4% in severe compression wood of conifers (Yamamoto et al. 1991). Our swelling experiments caused deformations in the same range or higher deformations than released strains measured in standing trees. Even though individual cells, tissue

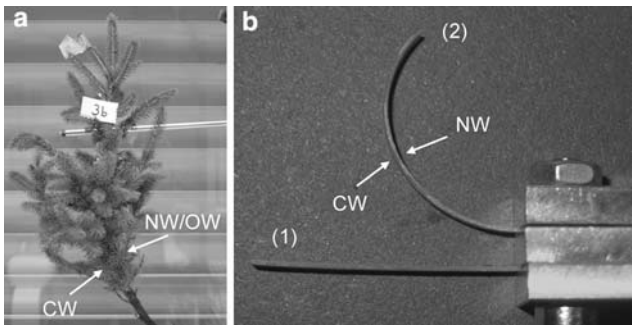

Fig. 6 **a** Leaning conifers upright when compression wood cells (*CW*) and normal wood cells (*NW*) (or rather opposite wood, *OW*) are deposited on opposite sides of a trunk (or branch). **b** (*1*) a straight bilayer consisting of a normal wood and a compression wood tissue with water-saturated cell walls (*2*) bends due to swelling with sodium iodide because compression wood cells tend to elongate and normal wood cells tend to shorten upon swelling leading to a net bending stress

sheets and small bulk wood samples may deform to a greater extent than the entire wood of a trunk, the data indicate that a simple swelling process may already be sufficient to incorporate internal stresses within the tissues.

The swelling process could be simulated in a model system of lignified cell wall materials using sodium iodide. Therefore it seems possible that the salt treatment leads to a swelling of the cell wall as originally caused by lignin incrustation during the differentiation process (Boyd 1950b). Or speculatively, cell death and incorporation of internal stresses in the cell wall take place simultaneously in a way that the cell wall may swell spontaneously while the protoplast is disintegrating. However, to clarify these hypotheses, so far too little is known about the processes of formation of secondary cell walls, their hygroscopicity and their potential for swelling in the course of the differentiation of tracheids.

We have demonstrated in both empirical studies and theoretical considerations that the wood cell behaves as an actuator upon swelling with a movement solely governed by the cells internal architecture. Therefore, a simple swelling mechanism might be sufficient to enable conifers to generate tensile or compressive forces as needed. As shown in Fig. 6 in a simple model system, this principle might well be considered also for artificial microactuators (Watanabe et al. 2002; Ikeda et al. 2003) as an enhancement of anisotropic polymer gels by a bio-inspired fibre-reinforcement.

Acknowledgments This paper is dedicated to Prof. Takashi Okuyama, University of Nagoya, Japan, who passed away in a car accident in November 2004. We thank the Max Planck Society and the Fonds zur Förderung der wissenschaftlichen Forschung (FWF), Austria, for financial support. We are grateful to Ingrid Zenke and Oskar Paris, Max Planck Institute of Colloids and Interfaces, for determining cellulose microfibril angles.

References

Bamber RK (1979) The origin of growth stresses. Forepride Digest 8:75–79 and 92

Boerjan W, Ralph J, Baucher M (2003) Lignin biosynthesis. Annu Rev Plant Biol 54:19–46

Boyd J D (1950a) Tree growth stresses I: growth stress evaluation. Aust J Sci Res Ser B Biol Sci 3:270–293

Boyd JD (1950b) Tree growth stresses III: the origin of growth stresses. Aust J Sci Res Ser B Biol Sci 3:294–309

Braam J (2005) In touch: plant responses to mechanical stimuli. New Phytol 165:373–389

Burgert I, Gierlinger N, Zimmermann T (2005) Properties of chemically and mechancially isoalated fibres of spruce (*Picea abies* [L.] Karst.). Part 1: Structural and chemical characterisation. Holzforschung 59:240–246

Burgert I, Okuyama T, Yamamoto H (2003) Generation of radial growth stresses in the big rays of konara oak trees. J Wood Sci 49:131–134

Carlsson LA, Pipes RB (1989) Hochleistungsfaserverbundwerkstoffe. BG Teubner Verlag, Stuttgart

Côte WA, Day AC (1965) Anatomy and ultrastructure of reaction wood. In: Côte WA (eds) Cellular ultrastructure of woody plants. Syracuse University Press, NY, pp 391–418

Dawson C, Vincent JFV, Rocca AM (1997) How pine cones open. Nature 390:668

Färber J, Lichtenegger HC, Reiterer A, Stanzl-Tschegg S, Fratzl P (2001) Cellulose microfibril angles in a spruce branch and mechanical implications. J Mat Sci 36:5087–5092

Fahlén J, Salmén L (2005) Pore and matrix distribution in the fiber wall revealed by atomic force microscopy and image analysis. Biomacromolecules 6:433–438

Fengel D, Wegener G (1984) Wood—chemistry, ultrastructure, reactions. De Gruyter, Berlin

Forterre Y, Skotheim JM, Dumais J, Mahadevan L (2005) How the venus flytrap snaps. Nature 433:421–425

Fratzl P, Burgert I, Keckes J (2004) Mechanical model for the deformation of the wood cell wall. Z Metallkd 95:597–584

Gierlinger N, Schwanninger M (2006) Chemical imaging of poplar wood cell walls by confocal Raman microscopy. Plant Physiol 140:1246–1254

Ikeda T, Nakano M, Yu Y, Tsutsumi O, Kanazawa A (2003) Anisotropic bending and unbending behavior of azobenzene liquid-crystalline gels by light exposure. Adv Mater 15:201–205

Keckes J, Burgert I, Frühmann K, Müller M, Kölln K, Hamilton M, Burghammer M, Roth SV, Stanzl-Tschegg SE, Fratzl P (2003) Cell-wall recovery after irreversible deformation of wood. Nat Mater 2:810–814

Kollmann F (1982) Technologie des Holzes und der Holzwerkstoffe, 2nd edn. Springer, Heidelberg

Kubler H (1987) Growth stresses in trees and related wood properties. For Prod Abstr 10:31–119

Lichtenegger H, Reiterer A, Stanzl-Tschegg SE, Fratzl P (1999) Variation of cellulose microfibril angles in softwoods and hardwoods—a possible strategy of mechanical optimization. J Struct Biol 128:257–269

Mattheck C, Kubler H (1996) Wood—the internal optimization of trees. Springer, Heidelberg

McMahon TA (1973) Size and shape in biology—elastic criteria impose limits on biological proportions, and consequently on metabolic rates. Science 179:1202–1204

Niklas KJ, Spatz H-C (2004) Growth and hydraulic (not mechanical) constraints govern the scaling of tree height and mass. Proc Natl Acad Sci USA 101:15661–15663

Reiterer A, Lichtenegger H, Tschegg S, Fratzl P (1999) Experimental evidence for a mechanical function of the cellulose microfibril angle in wood cell walls. Philos Mag A 79:2173–2184

Spatz H-C, Köhler L, Niklas KJ (1999) Mechanical behaviour of plant tissues: composite materials or structures? J Exp Biol 202:3269–3272

Timell TE (1982) Recent progress in the chemistry and topochemistry of compression wood. Wood Sci Technol 16:83–122

Wardrop AB (1965) The formation and function of reaction wood. In: Côte WA (ed) Cellular ultrastructure of woody plants. Syracuse University Press, NY, pp 371–390

Watanabe T, Akiyama M, Totani K, Kuebler SM, Stellacci F, Wenseleers W, Braun K, Marder SR, Perry JW (2002) Photoresponsive hydrogel microstructure fabricated by two-photon initiated polymerization. Adv Funct Mater 12:611–614

Yamamoto H (1998) Generation mechanism of growth stress in wood cell walls: roles of lignin deposition and cellulose microfibril during cell wall maturation. Wood Sci Technol 32:171–182

Yamamoto H, Okuyama T, Yoshida M, Sugiyama K (1991) Generation process of growth stresses in cell walls III: growth stress in compression wood. Mokuzai Gakkaishi 37:94–100